International Journal of Paleopathology 33 (2021) 209–219

Contents lists available at ScienceDirect

International Journal of Paleopathology

journal homepage: www.elsevier.com/locate/ijpp

Do computed tomography findings agree with traditional osteological examination? The case of porous cranial lesions

Amy S. Anderson [a,*], M. Linda Sutherland [b], Lexi O'Donnell [c], Ethan C. Hill [d], David R. Hunt [e], Aaron D. Blackwell [f], Michael D. Gurven [a]

[a] Department of Anthropology, University of California Santa Barbara, Santa Barbara, CA, 93106, USA
[b] MemorialCare, 17360 Brookhurst Street, Fountain Valley, CA, 92708, USA
[c] Department of Sociology and Anthropology, University of Mississippi, Oxford, MS, 38677, USA
[d] Division of Physical Therapy, Department of Orthopaedics and Rehabilitation, University of New Mexico School of Medicine, Albuquerque, NM, 87106, USA
[e] Department of Anthropology, National Museum of Natural History, Smithsonian Institution, Washington, DC, 20013-7012, USA
[f] Department of Anthropology, Washington State University, Pullman, WA, 99164-4910, USA

ARTICLE INFO

Keywords:
Radiology
Paleoimaging
Porotic hyperostosis
Cribra orbitalia
Anemia

ABSTRACT

Objective: The current study evaluates the feasibility of using clinical cranial computed tomography (CT) scans for assessing the presence and morphology of porous cranial lesions (cribra orbitalia, porotic hyperostosis).
Methods: Observers (n = 4) conducted three independent evaluations of porous cranial lesions based on photographs, 2-D CT, and 3-D CT scans of archaeological crania. Evaluations of the crania from each viewing scenario were compared to findings from direct macroscopic observation.
Materials: Twenty-two complete adult crania from the Peruvian sites of Pachacamac and Chicama.
Results: We found that lesion visibility differed by location: vault lesions with porosity larger than the resolution of the CT scan were identifiable across all viewing scenarios, but orbital lesions were identifiable only when extensive porosity was accompanied by widening of the inter-trabecular spaces. Lesions in stages of advanced remodeling were not visible on CT.
Conclusions: Paleopathological criteria applied to head CTs from clinical cases of suspected cranial fracture can reliably identify moderate to severe porous cranial lesions in living individuals.
Significance: This validation study opens the door to broader study of porous cranial lesions in living individuals that can address open questions about the causes and consequences of these commonly reported skeletal indicators of stress.
Limitations: Performance of all viewing scenarios was evaluated relative to assessment data from direct observation of skeletal remains, but direct observation is itself subject to error.
Suggestions for Further Research: The increasing resolution of routine CTs makes it increasingly possible to explore skeletal lesions in clinical contexts.

1. Introduction

1.1. Medical imaging and osteological inference

When paleopathologists diagnose a disease in human skeletal remains, they do so using operational definitions of the potential diagnoses, or 'skeletal disease scripts' (Mays, 2020). These operational definitions consist primarily of bone changes observed in clinical cases for which diagnoses are made independent of skeletal observations (Waldron, 2009) and sometimes of bone changes inferred from a biological approach to pathophysiology (Mays, 2012; Ortner and Ericksen, 1997). Such a diagnosis-centered approach is indispensable to paleopathological practice and an inextricable part of the traditional relationship between paleopathology and the clinical sciences (Mays, 2012). However, advances in medical imaging, particularly in computed tomography (CT), have made it possible to create 3-D reconstructions of the skeletal surface that parallel the archaeologist's direct view of human skeletal remains. This parallelism opens the door to a logical reversal—rather than asking which skeletal changes are associated with a given diagnosis, a lesion-centered approach asks which aspects of

* Corresponding author.
E-mail address: amy_anderson@ucsb.edu (A.S. Anderson).

https://doi.org/10.1016/j.ijpp.2021.04.008
Received 24 December 2020; Received in revised form 10 April 2021; Accepted 24 April 2021
1879-9817/Published by Elsevier Inc.

disease are associated with a given lesion.

Mapping the relationship between skeletal manifestations of disease and the lived experience of individuals remains a critical endeavor for paleopathology (DeWitte and Stojanowski, 2015; Mays, 2012; Wood et al., 1992), one that can be productively addressed with examinations of skeletal lesions in contemporary cases. Existing clinical CT scans, with accompanying data on symptoms and diagnoses, stand to clarify lesion formation processes and the relationship between skeletal plasticity and individual experiences of disease. Not only will these investigations uncover the clinical implications of specific skeletal lesions but also extricate how severity of stress, age of onset, and comorbidities contribute to differences in lesion expression.

In order to bring osteological perspectives to clinical contexts, we first need to ascertain how well paleopathologically-defined features can be detected with medical imaging and how their expression in medical imaging might differ from that directly observed in skeletal materials. This ensures that clinical and archaeological investigation are not miscommunicating due to 1) differing definitions of skeletal phenomena or 2) constraints on the sensitivity of diagnostic imaging. The current study validates—and delineates the limitations of—a CT-based approach to evaluating porous cranial lesions on clinical CT scans with bone-optimized reconstructions.

1.2. Porous cranial lesions: A case study

Porous cranial lesions in the orbits and cranial vault (cribra orbitalia and porotic hyperostosis, broadly defined) are often used by bioarchaeologists as skeletal indicators of childhood physiological stress (O'Donnell, 2019; Obertova and Thurzo, 2004; Steckel et al., 2002). They present a good validation case because they are primarily archaeological phenomena, both in definition and in representation. Their frequency in the archaeological record far exceeds reports of their presence in clinical literature (Józsa and Pap, 1990; Stuart-Macadam, 1987). This disparity between the archaeological record and clinical literature is surprising since the social and environmental factors that bioarchaeologists link to these skeletal lesions include chronic microbial and parasitic infection, food insecurity, and inadequate dietary diversity, all of which are still common on a global scale (Ortner, 2003; Rivera and Mirazon Lahr, 2017; Stuart-Macadam, 1987; Walker et al., 2009). The higher prevalence of porous cranial lesions reported in anthropological studies of modern mortality samples suggests that the absence of these lesions reported in clinical contexts may not reflect their absence in contemporary populations (Beatrice and Soler, 2016; David, 2018; O'Donnell et al., 2020; Steyn et al., 2016; Wright and Chew, 1998). Here we evaluate the feasibility of applying paleopathological criteria to CT scans for porous cranial lesion identification - an approach that could lead to different conclusions about the prevalence of these skeletal lesions in contemporary populations and to new insights on their causes and consequences.

1.3. Archaeological and radiological approaches to porous cranial lesions

The different methods by which osteologists and radiologists examine the skeleton can emphasize different aspects of lesion-related morphology (Mays, 2012). Because osteologists largely define and identify porous cranial lesions based on direct macroscopic examination of the ectocranial surface they tend to emphasize surface porosity, while radiologists have historically viewed the cranium on radiographs in the sagittal or coronal plane and focused instead on expansion of the bone layers in the cranial vault. The main clinical radiological finding equated with porous cranial lesions is a radially striated 'hair-on-end' appearance of the diploic trabeculae with abnormal thickness of the diploë. This finding is noted in radiography of severe childhood anemias, most commonly thalassemia and sickle-cell anemia (Angel, 1964; Resnick and Niwayama, 1988). These anemia-related skeletal changes are initiated in the diploic space; cranial surface porosity that results from anemia should thus always be accompanied by underlying diploic changes.

The cranial porosity encountered in archaeological cases is caused by multiple lesion formation processes, marrow hyperplasia being just one. Radiological and histological examination of archaeological skeletal remains reveals that cranial surface porosity is not invariably accompanied by expansion of the underlying diploic bone (Brickley, 2018; Ortner, 2003). Histological cross sections from archaeological cases of porous cranial lesions confirm variation in underlying morphology that speaks to the range of processes capable of producing a porous appearance of the ectocranial surface (Brickley et al., 2020; Ortner, 2003; Wapler et al., 2004). It is also clear, given the age distribution of unremodeled lesions in the archaeological record, that these lesions form almost exclusively in childhood, and that lesions in adults are largely evidence of individual medical history (Blom et al., 2005; Stuart-Macadam, 1985). Of course, lesions comprised of new bone formation in response to localized inflammation need not be confined to childhood, though the higher rate of bone turnover during growth and development makes osseous responses to stimuli more likely at younger ages.

Stuart-Macadam's (1987) radiological study identified a suite of radiological features that are more commonly seen in radiographs of crania with porous vault and orbital lesions. Taken in aggregate, these lesion-associated traits suggest that marrow hyperplasia is a cause of porous cranial lesions but likely not the cause of all such lesions in the study. The only feature common to the majority of lesion cases—an abnormal texture of the diploë described as 'diploic granularity'—was also the least specific and deemed the most difficult trait to evaluate. The hair-on-end feature was pathognomonic for porous cranial lesions but rare, only found in 8% of lesion cases examined by Stuart-Macadam.

We propose that the causes and consequences of porous cranial lesions in the living be investigated by applying paleopathological criteria for their identification to clinical cranial imaging. Rather than identifying these lesions in living individuals based primarily on anemia-related changes in the diploic space, cranial surface porosity might be investigated as a phenomenon in its own right. Its associations with underlying osseous abnormality, clinical diagnoses, and individual disease experience can then be examined. Advances in medical imaging technology, particularly computed tomography, make it possible to realize this approach (Exner et al., 2004; Naveed et al., 2012; Rivera and Mirazon Lahr, 2017).

Cranial computed tomography (CT) provides more detailed images than traditional radiographs. Rather than the single superimposed image produced by radiography, CT affords both three-dimensional views of the skull's ectocranial surface and discrete cross sections in axial, coronal, and sagittal planes (Beckett, 2014). Cranial surface porosity, underlying osseous features, and their relationship both to each other and to disease can thus be investigated using CT reconstructions. Paleopathologists have already used CT to differentiate causes of cranial vault lesions (Zuckerman et al., 2014) and test the relationship between causes of orbital and vault lesions (Rivera and Mirazon Lahr, 2017). Applying a lesion-centered approach to CT scans of living individuals is a natural extension of this research and opens new possibilities for exploring the connection between porous cranial lesions and individual disease experience. A ready pool of data for such studies exists in scans obtained during medical treatment.

As a first step toward investigating these lesions in contemporary populations, we assess the comparability of cranial lesion data produced using traditional in-person and photo-based osteological evaluations of crania and evaluations of the same crania using multiple CT viewing scenarios. Following in-person evaluation by lead author (ASA) of 22 archaeological crania for lesion presence and lesion surface morphology, four observers (including ASA) conducted independent evaluations of porous cranial lesions using the same crania based on photographs, 3-D CT reconstructions of the cranial surface, and cross-sectional 2-D CT views. In cross section, observers primarily recorded pitting and porosity at the ectocranial surface to evaluate the utility of 2-

D cross-sectional views for capturing the surface features that define porous cranial lesions in archaeological settings.

2. Materials and methods

2.1. Subjects

This study utilized crania housed at the Smithsonian National Museum of Natural History (NMNH) biological anthropology collection. Because this study was intended to establish a baseline for an analysis of porous cranial lesions from existing CT scans of living adults, we focused solely on adult crania. Adult status was determined by the presence of fully erupted third molars, evidential wear on the dentition, and closure of late adolescent apophyses. Eligible crania selected were >90 % complete. Individuals with extreme cranial modification or excessive taphonomic degradation were excluded from analysis. Crania were chosen to represent the range of bilateral porous cranial lesions expressed in adults (see Fig. S1).

The study sample consisted of 22 adult crania (15 estimated male) collected by Aleš Hrdlička in 1913 (Hrdlička, 1914). All but one came from the site of Pachacamac (A.D. 200–1533) on the central Peruvian coast. The final individual, selected for their extreme cranial vault lesions, was from the Chicama valley, 685 km north of Pachacamac. Broad age categories were estimated based on dental wear and ectocranial suture closure (Meindl and Lovejoy, 1985), and sex was estimated from cranial nonmetric features (Buikstra and Ubelaker, 1994).

2.2. CT scanning

Scan parameters and subject positioning were selected to approximate those used for brain CT scans of living patients. Scanning was implemented using the NMNH Siemens SOMATOM Emotion 6 computed tomography (CT) scanner with 0.63 mm slice thickness, 130 kVp, 140 mAs (Table 1). Scans were obtained with a pitch of 0.65. Image resolution in the axial plane was determined by the scan's field of view (199 mm) and the 512 × 512 scan matrix, producing pixels approximately 0.39 mm^2. Slice thickness constrained image resolution in the Z plane, creating coronal and sagittal images with pixels 0.39 mm x 0.63 mm. Each cranium was positioned in Frankfort plane (to replicate living patient positioning), the midline centered on nasion. Siemens ultrasharp U90 bone reconstruction algorithm (kernel) was applied to the raw data to optimize visualization of skeletal structures. In clinical contexts, such an algorithm would typically be used to assess skull trauma in tandem with a standard soft-tissue algorithm to identify intracranial hemorrhage (Maetani et al., 2016).

2.3. Cranial lesion evaluation

2.3.1. In-person lesion classification

Lesion presence and morphology were classified in person by ASA using the Stuart-Macadam (1985) classification schema (see Figure S1): 0 – absence of lesion; 1 – scattered fine foramina; 2 – large and small isolated foramina; 3 – foramina coalescing in a trabecular structure; 4 – outgrowth in trabecular structure from the normal contour of the outer bone table. When morphology varied within a single lesion, the highest score was recorded. Of the six cases of ectocranial vault lesions classified as 3, four presented with well-healed superficial coral-like impressions, while in the other two cases coalescing foramina perforated the outer table.

2.3.2. Photograph and CT-based lesion classification

Four observers—three osteologists familiar with porous cranial lesions (ASA, LO, EH), and an experienced clinical radiologist (MLS)—scored the crania for porous lesions of the orbital roofs and cranial vault using three separate viewing scenarios: photographs, 2-D orthogonal CT multi-planar reconstructions (MPR), and 3-D CT volume renderings. Order of crania was randomized for each observer at each observation session. Photographs were assigned anonymized identifiers to limit

Table 1
A selected lexicon of CT terminology.

	Term	Synonyms	Definition	Importance
Setting scan parameters	Gantry	–	The circular frame housing the x-ray tube, collimators, and detectors	Positioning of the gantry relative to the patient determines the angle of scan acquisition.
	Pitch	Increment; table feed	Distance traveled by the scanner table in one 360° gantry rotation divided by beam width	Pitch determines how much interpolation is done to construct slices from helical CT. Lower pitch = higher image resolution. Higher pitch = lower resolution.
	Slice thickness	–	Depth in the Z axis (usually axial) of each constructed CT image	Slice thickness determines image resolution in coronal and sagittal reconstructions.
	Field of View (FOV)	–	Diameter of the area being scanned	Field of view (mm) divided by the size of the scan matrix (often 512) yields the image resolution (mm/pixel) in the axial plane. FOV can often be set prior to scanning, and smaller FOV results in higher resolution images.
	kilovoltage peak (kVp)	–	Maximum voltage of x-ray tube	Higher voltage can return higher image quality, but also results in higher radiation exposure to the patient.
	Milliamperes (mA)	–	Measure of the current in the x-ray tube	Like kVp, higher mA can return higher quality images, but this must be balanced against the need to minimize patient radiation exposure.
	Voxel	–	a cubic unit equivalent to a pixel for 3-D graphics	Voxel size is determined by axial resolution and slice thickness (0.39 × 0.39 × 0.625, in the case of this study). When slice thickness = axial resolution, voxel dimensions are cubic (isotropic) and image resolution in axial, coronal, and sagittal planes is identical.
Viewing scan reconstructions	Reconstruction algorithm	reconstruction kernel; filter; convolution algorithm	A filter that modifies CT projection data in order to reduce image blurring of backprojected 2-D images	Algorithms are chosen at the time of scanning based on the purpose of the scan. Those optimized for viewing bone (hard/sharp algorithms) produce sharper images with higher spatial resolution but can create higher density values at borders where density contrasts are high (edge hardening).
	Window Width	–	The range of CT density values mapped onto the shade palette of the CT image display	Setting the window width and level to the appropriate values can maximize visual differentiation for the tissue of interest while minimizing visibility of other tissue types.
	Window Level	–	The CT density value mapped to the middle tone of the CT display palette	

(Conlogue et al., 2020).

recognition of individual specimens across modalities, and CT observation sessions for 2-D MPR and 3-D volume rendering were conducted on separate days.

CT scans were evaluated using the freeware DICOM viewer Horos version 4.0.0 (Horos, 2019). In 2-D MPR the viewing window was set to Horos' bone-optimized preset, and observers were able to scroll through cross-sectional slices of the scan in coronal, sagittal, or axial planes. For 3-D volume rendering, observers were able to rotate volume-rendered images, and each observer chose settings within Horos that they deemed best to maximize detail visibility. While this introduces extra variables to evaluations from the 3-D renderings, it is also likely to capture a realistic source of variation in the way this viewing modality is used by different individuals and on different display screens. All observers chose to view renderings at the finest level of detail and best possible resolution and set the rendering colors to either 'VR muscle and bone' or 'VR bone.' Observers differed in their choices of preset window width and level settings ('Default,' 'Full Dynamic,' 'Bone CT'), voxel opacity function (logarithmic or linear), and individually customized shading settings (see Figs. S2 and S3).

In both photographs and CT 3-D volume rendering, observers scored lesion surface morphology using Stuart-Macadam's (1985) scoring classification. Observers did not score degree of lesion healing; no individual in the sample (all adults) appeared to have unremodeled lesions at time of death. On 2-D MPR images observers determined the presence or absence of three lesion-related traits (Fig. 1): superficial pitting of the outer table (ectocranial pitting), porosity of the outer table, and radial trabecular orientation (radiologic 'hair-on-end' appearance). For orbital roofs, observers scored only cortical porosity.

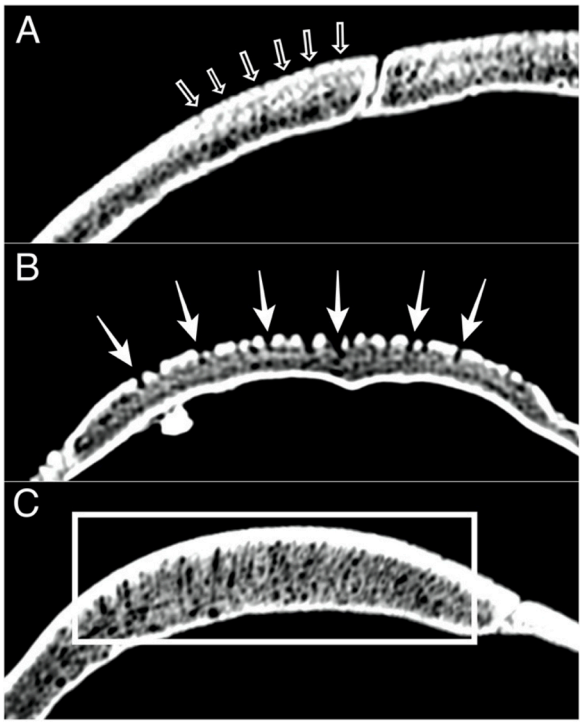

Fig. 1. Lesion-related traits as seen on 2-D CT MPR. A) Open arrows indicate ectocranial pitting: Dimples or divots disrupt the contour of the outer table's ectocranial surface (sagittal view, frontal and parietal bones). B) Solid arrows indicate porosity: porous channels run from the ectocranial surface to the diploic bone beneath the outer table (axial view, occipital bone). C) Hair-on-end appearance: Bone in the diploic space has a radial orientation with trabeculae lying perpendicular to the outer table. Note ectocranial pitting also visible in C (sagittal view, frontal and parietal bones).

3. Results and discussion

Lesion morphology scores were correlated among in-person, photographic, and 3-D CT assessments (Fig. 2), though each viewing modality has its own strengths and weaknesses for evaluating lesions, and the effect of viewing modality differed for vault lesions and orbital roof lesions (Table 2). The performance of each viewing modality was impacted by differences in image resolution and the depth or superficiality of lesion-related changes. For example, the high resolution of photographs relative to CT reconstructions resulted in higher correlation between photo-based and in-person evaluations of lesion morphology (Table 3). On the other hand, because features smaller than the scan resolution were not visible, pseudopathological features were often not rendered, and thus CT returned better agreement with direct observations of vault lesion presence/absence (Table 4). Evidence of vault lesions was clearest in CT viewing modalities when true porosity penetrated the full depth of the outer cortex (Fig. 1B). However, 3-D volume-rendered CT was more sensitive than 2-D MPR for detecting the shallower imprints of ectocranial pitting, and superficial osseous changes were visible only in photographs.

The range of lesion morphology visible on CT is delineated below. Using the scan parameters of the current study, porosity is most likely to be visible on cranial CT if surface diameter of individual foramina exceeds 0.4 mm or remodeling has not begun to obscure any underlying pathway from the diploë to the ectocranial surface. Due to scanning artifacts in the orbits, orbital roof lesions are difficult to identify unless surface porosity is accompanied by enlarged intertrabecular spaces. Because the effect of CT on evaluations of cranial vault lesions differs from its effect on orbital roof lesions, the effects of viewing modality on lesion visibility are discussed separately for vault and orbital lesions.

3.1. Cranial vault lesions

3.1.1. 3-D volume-rendered CT

Evaluations from 3-D volume-rendered CT out-performed 2-D MPR and photographs in detecting the presence of cranial vault lesions; observer consensus on 3-D volume-rendered CT images provided the closest match to in-person evaluation of cranial vault lesion presence (83 % agreement) (Table 4). The cranial surface reconstruction of 3-D volume-rendered CT also has the advantage over 2-D MPR of allowing observers to evaluate lesion morphology using the same criteria as direct observation of skeletal remains, though morphology scores from 3-D volume-rendering tend to be influenced by the same factors that affect lesion visibility.

Lesion visibility appeared to be determined by two features: the extent of true porosity and the size of cortical defects (pitting or porosity). The majority of observers agreed that cranial vault lesions were present on 3-D volume-rendered CT images when lesions manifest either as coalescing porosity (score: 3 or 4) or included foramina with a diameter larger than the scan resolution (Fig. 3). Foramina above this size threshold ($>$ 0.4 mm) were identified as 'large foramina' (score: 2) from photographs and in-person observation (Fig. 4A) but often identified on 3-D CT images as 'fine scattered foramina' (score: 1). Of the 15 crania with in-person vault lesion scores $>$1, observers unanimously identified lesions in 13 on 3-D CT. Observer disagreement over the remaining two crania was likely due to the advanced state of lesion remodeling; superficial impressions lacking open porosity created ambiguous lesion expression on CT images. Altogether, these results suggest that vault lesions with more than superficial involvement and porosity surpassing the scan resolution can be identified on CT scans of living individuals.

3.1.2. CT 2-D MPR

2-D MPR evaluations had the lowest sensitivity of all viewing modalities (0.63) for detecting cranial vault lesions but the highest specificity (0.75). Accordingly, one may be fairly confident that lesions

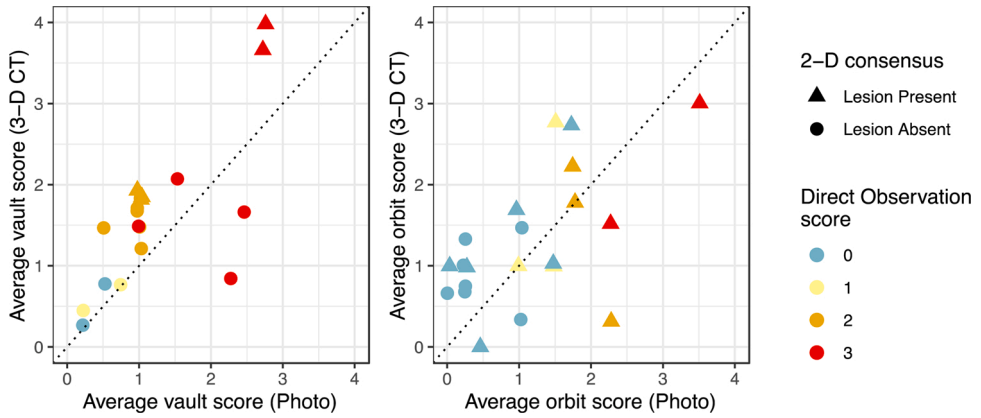

Fig. 2. Comparison of lesion evaluations for each cranium (n = 22) across all viewing scenarios: in-person cranial lesion classification (color scale), average cranial lesion scores from four observers based on evaluation of photographs (x-axis) and based on 3-D volume rendering (y-axis), and majority opinion on lesion presence/absence from 2-D MPR (shape scale).

Table 2
Results of ordered logistic regression model showing that the effect of viewing modality on lesion morphology reporting differs for orbital and vault lesions, particularly for CT.

	Odds Ratio	lower 95 % CI	upper 95 % CI
Modality Photo	1.17	0.74	1.87
Modality3-D CT	0.49	0.30	0.78
Lesiontype_orbit	0.12	0.07	0.20
modalityphoto:lesiontype_orbit	2.02	1.01	4.07
Modality3-D CT:lesiontype_orbit	6.61	3.23	13.61

Reference case is direct observation of vault lesions. Vault lesions are likely to be given lower scores from 3-D CT than from direct observation, while orbital lesions are likely to be given higher scores. Lesion classification categories were treated as a heuristic ordinal scale for this model. The model was estimated in R v. 3.6.1 (http://cran.r-project.org/) using the *polr* command in the *MASS* package.

Table 3
Relative performance of photographs and volume-rendered (3-D) CT images for determining lesion morphology category (0-4).

	Vaults		Orbits	
	Photo	3-D	Photo	3-D
Mean score difference (relative to Direct Obs.)	1.30	−0.22	1.44	0.63
Pearson's R (correlation with Direct Obs.)	0.78 (0.68, 0.85)	0.59 (0.43, 0.71)	0.67 (0.53, 0.77)	0.32 (0.11, 0.51)
Intraclass Correlation Coefficient (95 % ***Confidence Interval)***	0.80 (0.66, 0.90)	0.66 (0.46, 0.82)	0.58 (0.37, 0.77)	0.27 (0.04, 0.61)

Intraclass Correlation Coefficients show interobserver concordance within each viewing modality.

identified as present from MPR are indeed present but expect a high frequency of false negatives. In light of the relatively low sensitivity of MPR for identifying lesion presence, it seems likely that the traditional planar view of crania in radiological examinations has contributed to the under-identification of porous cranial lesions in clinical settings, as ectocranial pitting is often the primary feature of remodeled lesions. Observer evaluation of 3-D volume-rendered CT appears to be more sensitive than 2-D MPR for detecting surface features of the outer table such as ectocranial pitting. Despite 2-D MPR's low sensitivity for identifying lesions based on surface features, it provides valuable views of the extent and nature of lesion-related changes below the ectocranial surface and is thus indispensable to CT-based evaluations of porous cranial lesions.

Differences in observer agreement across lesion-related traits illuminate 2-D MPR's strengths and weaknesses. Observer agreement on presence/absence of true porosity was higher than agreement on ectocranial pitting. All agreed that true porosity was present in two crania and absent in 13 cases. This low frequency of true porosity demonstrates the extent of lesion healing in the study sample (see Mensforth et al., 1978 for a description of stages of healing in porous cranial lesions), and the higher observer agreement for this trait suggests that 2-D MPR is better at capturing lesions with unremodeled porosity.

Observers also visually evaluated crania for the presence of radially oriented trabeculae in the diploic space, indicating the presence of radiological hair-on-end appearance (Fig. 1C). True to previous archaeological reports of hair-on-end, unambiguous hair-on-end was only found in cases with other pronounced lesion-related changes (n = 3). 2-D MPR's greatest advantage remains that, unlike other viewing modalities, it provides a window into lesion-associated changes below the cortical surface, making it a critical component of a CT-based evaluation even if 3-D volume-rendered images provide a more sensitive tool for lesion detection.

3.1.3. Photographs

Despite yielding higher interobserver agreement on lesion morphology (ICC = 0.80; CI 0.66−0.90) than 3-D volume-rendered CT (ICC = 0.66; CI 0.46−0.82), photo-based evaluations had, unexpectedly, worse agreement with in-person assessment of lesion presence/absence (sensitivity = 1, specificity = 0.10). Compared to in-person evaluations, photo-based evaluations over-reported lesion presence (Fig. 5A). While ASA reported absence of vault porosity in 27.3 % of crania during initial in-person evaluation, there was no case in which all observers agreed from photographs that vault porosity was absent. False positive cases from photo-based evaluations were primarily reported as scattered fine foramina (score: 1). We attribute this discrepancy to the fact that in-person lesion evaluations by ASA were conducted after selecting the study sample from a broader collection of skeletal material, providing an opportunity to calibrate expectations for postmortem damage in the Pachacamac remains. Photo-based evaluations are therefore more likely to misclassify taphonomic changes as pathological.

Volume-rendered 3-D CT images, on the other hand, have lower resolution than photographs, smoothing over surface features smaller than the scan resolution. The limitations of CT resolution render CT-based evaluations less prone to misidentifying postmortem surface erosion as pathological but also reduce the likelihood of recognizing subtler pathological features that are visible during traditional osteological examinations of dry bone. Nevertheless, even for in-person evaluations of skeletal remains, disagreement over the line between pathological and non-pathological expression is a recognized source of

Table 4
Relative performance of different viewing modalities for detecting lesion presence/absence.

Vault	Photo	2-D MPR	3-D
Sensitivity*	1	0.63	0.93
***Specificity**†*	0.10	0.75	0.5
Positive Predictive Value**	0.79	0.9	0.86
***Negative Predictive Value**††*	1	0.38	0.67
% Agreement with Direct Obs.	79.5	52.3	83.0
Orbits	**Photo**	**2-D MPR**	**3-D**
Sensitivity	0.94	0.97	0.69
Specificity	0.52	0.39	0.29
Positive Predictive Value	0.53	0.48	0.35
Negative Predictive Value	0.94	0.96	0.62
% Agreement with Direct Obs.	67.0	44.3	48.7

Sensitivity and specificity, used clinically to measure the accuracy of a diagnostic test in detecting a disease, are used here to describe the detection rates of cranial lesions from different viewing modalities. Values are calculated using the directly observed lesion frequencies as 'true' prevalence.

* $\frac{\text{number of lesions reported present}}{\textit{number of lesions truly present}}$.

† $\frac{\textbf{\textit{number of lesions reported absent}}}{\textbf{\textit{number of lesions truly absent}}}$.

** The probability a lesion identified as present was truly present (i.e., reported during direct observation):
$\frac{\textit{lesion frequency} * \textit{sensitivity}}{((\textit{lesion frequency} * \textit{sensitivity}) + (1 - \textit{lesion frequency}) * (1 - \textit{specificity})}$.

†† Probability that a case identified as absent of lesions was truly absent (i.e., similarly reported during direct observation):
$\frac{(1 - \text{disease frequency}) * \text{specificity}}{(\text{frequency} * (1 - \text{sensitivity}) + (1 - \text{frequency}) * \text{specificity})}$.

noise in osteological data (Ubelaker, 2003). Archaeologists occasionally avoid dealing with ambiguous cases by increasing the porosity threshold for considering pathological changes to be present (Lewis, 2017; Watts, 2013), a strategy that may create more comparable data on lesions in past and present populations (though lesion frequencies should never be compared directly – see Wood et al. (1992)).

3.2. Orbital roof lesions

Across all viewing modalities, only orbital roof lesions with coalescing foramina (in-person score: 3) were easily visualized. In these cases (n = 2), widening of the inter-trabecular spaces in the spongy bone of the orbital roof was clearly visible in 2-D MPR (Fig. 6), and the lesions

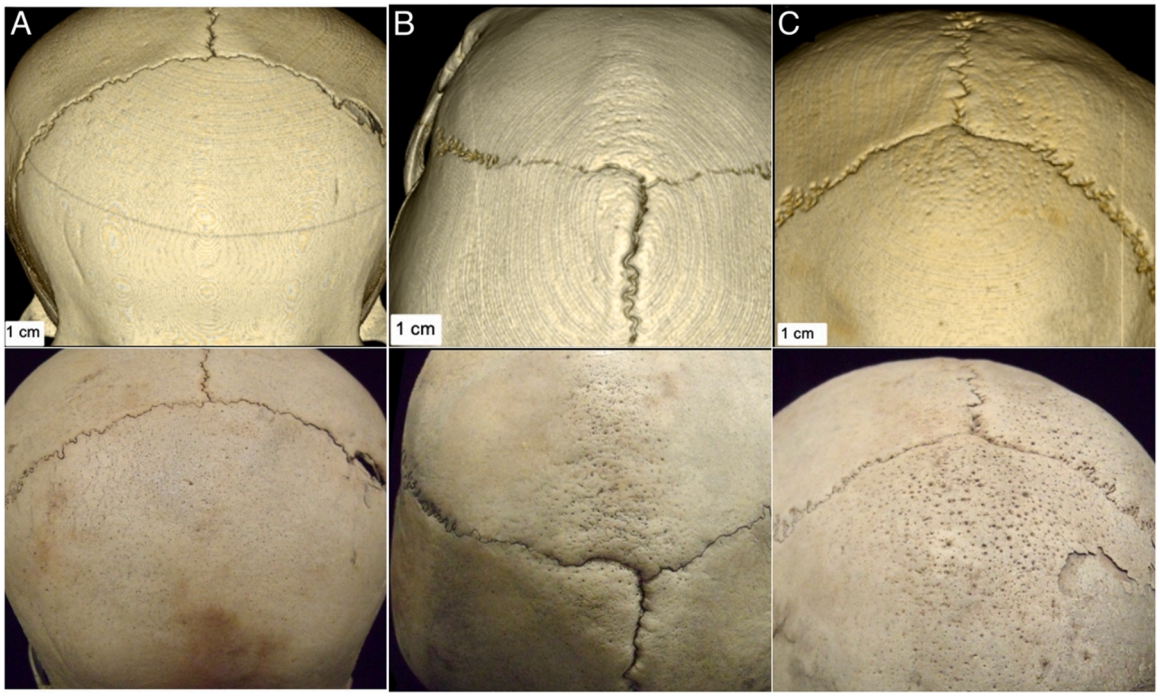

Fig. 3. Side-by-side comparison of ectocranial lesion visibility for three crania: photos (bottom) and 3-D CT volume renderings (top). A) Lesions classified from photographs as 1, 'scattered fine foramina,' were not well translated into 3-D CT renderings. B) Superficial ectocranial impressions created disagreement about lesion classification from photographs, and these superficial structures were not visible in 3-D CT renderings. C) Lesions scored from photographs as 2, 'large and small isolated foramina,' were consistently identified from 3-D CT renderings, though small foramina were often not visualized unless they occurred near bregma. The concentric rings visible on 3-D renderings are minor stair-step artifacts in the scans that result from mapping objects that lie obliquely across the axial plane of acquisition. Image reconstruction with smoothing algorithms will minimize these artifacts but also obscures fine cranial porosity. 'Fine scattered foramina' is also described by Buikstra and Ubelaker (1994) as 'barely discernible porosity,' (p.151) while 'large foramina' is alternately described as 'true porosity' (p.126), a distinction which seems appropriate to their appearance in volume-rendered CT images.

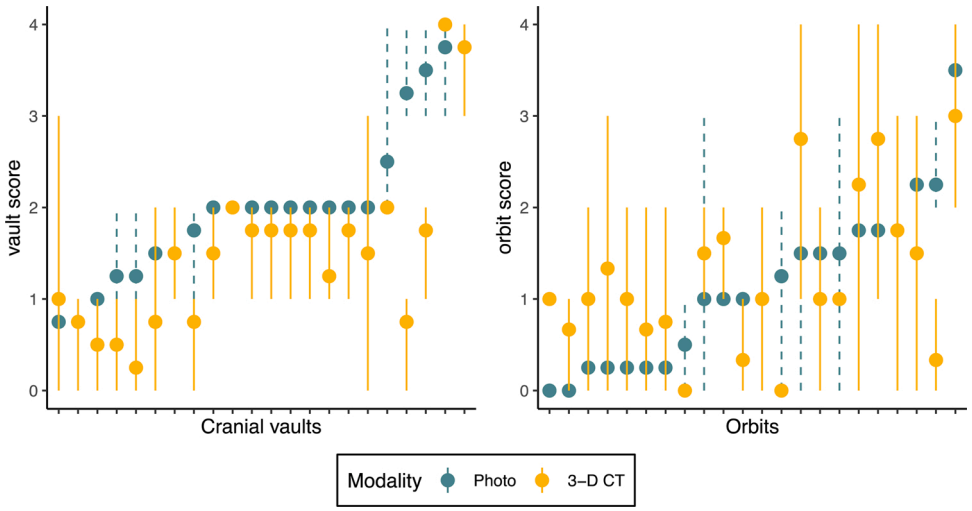

Fig. 4. Comparison of observer agreement within and between viewing modalities for a) vault lesions and b) orbital roof lesions. Each point is the average lesion score (n = 4 observers) for an individual cranium; vertical lines show the range of lesion morphology scores assigned to each cranium. Observations in each panel are ordered according to the mean photo-based score for the lesion of interest.

were easily and consistently identified as present in all viewing modalities. In contrast, observers were unable to agree, in any viewing scenario, whether lesions were present when orbital roofs displayed only isolated foramina or vascular impressions. As a whole, orbital roof lesions had high observer disagreement in all viewing modalities (Table 4; Table S1), but there is a clear threshold of lesion visibility for examining these lesions in living individuals: orbital roof lesions with widened inter-trabecular spaces can be identified on standard cranial CT scans.

3.2.1. *CT imaging*

In the absence of substantial trabecular bone in the orbital roof, CT reconstructions often introduce limitations on orbital roof visibility caused by CT artifacts that render gaps in the region of interest (Fig. 6B). These artifacts primarily result from the scan's failure to render the orbital roof due to the thinness of the frontal bone's horizontal plate and its oblique orientation relative to the axial acquisition of the CT scan. The failure to capture thin areas of the orbital roof led to over-

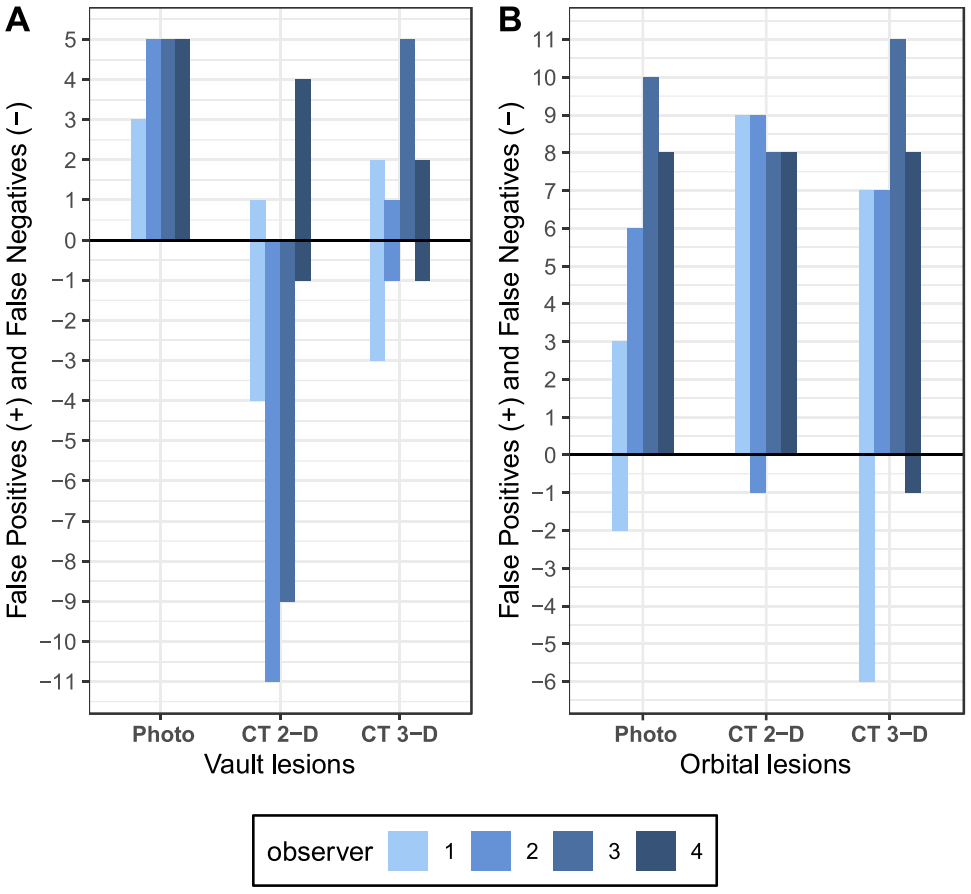

Fig. 5. Comparison of false positive and false negative lesion identification rates across viewing modalities, assuming that initial in-person evaluations of lesion presence/absence from direct observation are true. The positive values for each bar indicate the number of crania scored as absent of pathological condition during initial in-person evaluation that were thought to show evidence of lesions in subsequent observation sessions using different viewing modalities. The negative values indicate the number of crania identified as having lesions during in-person evaluation that were subsequently scored as absent of lesions. The length of each bar indicates the amount of deviation from in-person presence/absence evaluations, and the position of the bar indicates the direction of deviation. Note: Possible number of 'false' identifications is constrained by the lesion frequencies from in-person evaluations; vault and orbital values here should thus not be directly compared.

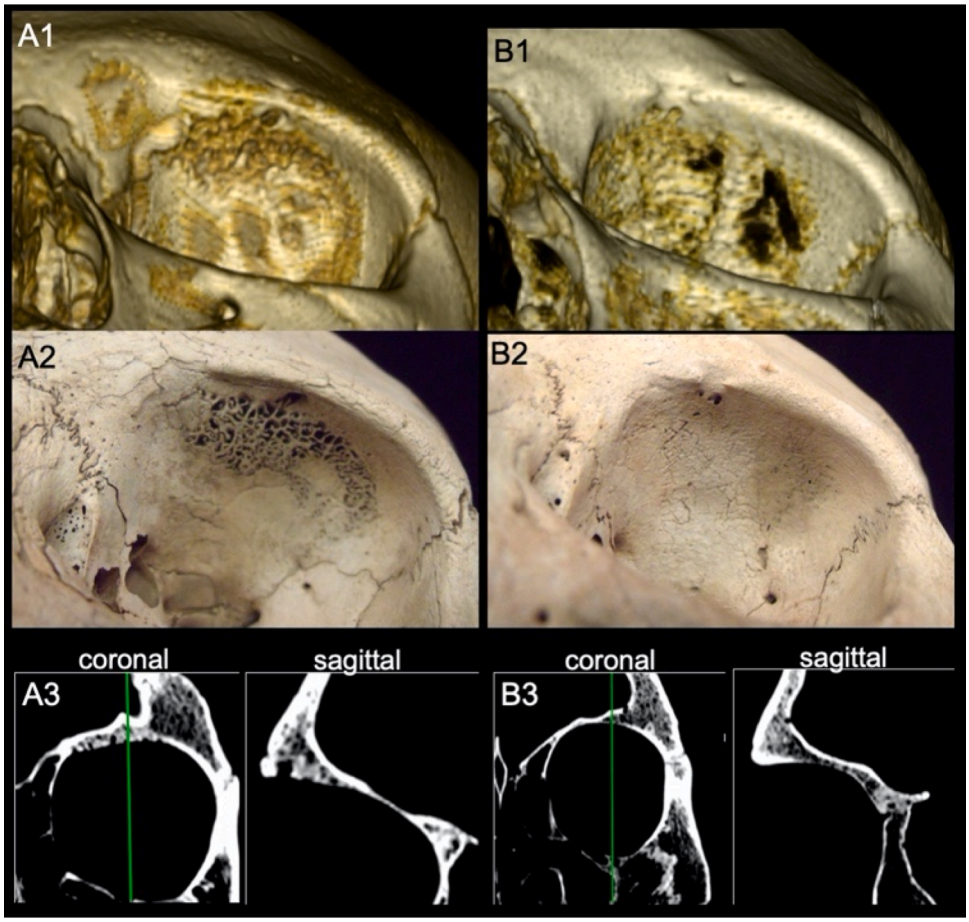

Fig. 6. Orbital roof lesions with skeletal changes indicative of marrow hyperplasia (A) are easily visible in all viewing modalities, but orbital roof porosity is often exaggerated in CT reconstructions (B).

identification of orbital roof porosity in CT viewing scenarios. When the orbital roof *was* visibly rendered, the axial scan acquisition caused a stairstep effect with visible slices in the volume-rendered orbit that resulted in observer uncertainty over subtler features such as isolated foramina and vascular impressions.

3.2.2. *Photographs*

Though photo-based evaluations yielded better interobserver agreement than CT and provided the closest match to in-person evaluations, observers disagreed on whether orbital lesions were present in almost half of photographic cases. A number of factors contribute to disagreement in identifying lesion presence or absence using traditional osteological methods and seem to pose particular difficulty in evaluating orbital roof lesions. For example, well-healed lesions can be difficult to identify in photographs, especially when there is variegated discoloration of the orbit. Plant roots can create postmortem discoloration in a vascular pattern. The appearance of non-pathological porosity varies with age, and the same sensitivity to porosity may not be appropriate for individuals of all ages. Dirt inclusions can make porosity difficult to assess, and lamellar bone deposition is hard to determine without in-person observation. Finally, the depth and curvature of the orbit itself poses a challenge for producing photographs with adequate clarity for evaluation of pathological conditions, though techniques like focus stacking can help address this issue (Clini et al., 2016). CT obviates most of these challenges, though CT-specific issues (see *3.2.1* above) take their place. Ultimately, minor deviations in orbital roof morphology are sources of observer uncertainty, regardless of viewing modality.

3.3. *Technical considerations: CT scanning parameters*

Phenomena of osteological interest are most feasibly investigated in living individuals using existing CT scans and accompanying medical data. Accordingly, it is important to define the limitations of skeletal lesion detection imposed by the scan parameters of routine cranial CTs. In clinical practice, CT acquisition parameters for standard head CT differ depending on the purpose of the scan. Scans obtained for assessing cranial fracture subsequent to head trauma are the most likely to have submillimeter slices appropriate for visualizing skeletal lesions, and these scans will include a reconstruction using a bone-optimized algorithm. The names and precise parameters of bone algorithms vary across scan manufacturers, but comparable settings do exist (see McCollough, 2011 for a guide). The caveat remains though, that all bone-optimized algorithms contain corrections for the artificially high density values that can appear at the edges of dense materials such as bone (beam hardening artifacts). Algorithms from different scanners vary in the weight of their beam hardening correction, and the extent to which this impacts the visibility of porous skeletal lesions is uncertain.

Previous investigation into the CT visibility of orbital roof lesions has recommended positioning crania "at a slice angle of 90° between the slice plane and the orbital roof" (Exner et al., 2004, p.170). Though this patient positioning optimizes visibility by avoiding CT artifacts and providing higher-resolution imaging of features in the orbital roof, it is rarely used in clinical CT protocols except in targeted investigations of orbital roof anomalies such as orbital tumors (Rosel, 2015). Head CTs obtained with the patient in a supine position are more common and are indicated for patients with a wider range of potential diagnoses. It may be prudent for a future study to assess the effect of variations in skull

positioning on the perceptibility of lesions. Positioning has not been found to affect cranial measurements from CT reconstructions (Hassan et al., 2009), but the visibility of submillimeter porosity may be more sensitive to minor changes in orientation of the skull.

CT slice thickness in the axial plane is a critical determinant of lesion visibility because it limits image resolution in the reconstructed sagittal and coronal planes. A slice thickness equal to the axial resolution (roughly 0.4 mm in a standard head scan) is achievable with 32- or 64-slice scanners, though 16-slice scanners get close (0.5−0.75 mm minimum slice thickness, depending on the scanner model) (Goldman, 2008). Six-slice scanners such as the Siemens Emotion 6 used here can also achieve submillimeter slices but are rarely used with such thin slices in clinical settings due to the longer scanning time required – a less important consideration for scanning skeletal remains.

With the thin slices available in newer scanners, the true limit on image resolution will be the scan's field of view (FOV). In all CT scanners, pixel resolution of axial slices is determined primarily by the scanner's beam width and the FOV, and FOV is determined by the size of the area to be scanned; all else equal, juvenile head CTs will have higher resolution—and better lesion visibility—due to the smaller FOV for smaller crania. The visibility of fine porosity on the superior aspect of the calvarium is thus unlikely to be much improved by incremental advances in scanning technology.

Pitch also influences the clarity of details in scan reconstructions, partly by influencing the minimum thickness of slices that can be constructed from helical scans. A pitch setting close to 1, which creates contiguous slices, has shown good results for viewing orbital roof lesions (Naveed et al., 2012), but scans obtained for viewing the intracranial space often have lower pitch settings designed to minimize the likelihood of scanning artifacts and maximize image resolution. The low pitch (0.65) setting for scans in this study, chosen to match parameters for existing brain CT, results in some smoothing of density values, particularly in the Z plane. This smoothing of the data likely obscures some finer porosity, and detection of surface porosity is probably less sensitive on the lateral portions of the calvarium due to the combination of smoothing and lower resolution in the Z plane (Maetani et al., 2016). Fortunately, porous lesions of the occipital bone, which might be most obscured by the resolution constraints set by slice width, tend to have larger foramina than lesions on other areas of the cranial vault. As mentioned earlier, the scan parameters of the current study are most likely to render cranial porosity if surface diameter of individual foramina exceeds 0.4 mm or remodeling has not begun to obscure any underlying pathway from the diploë to the ectocranial surface.

3.4. Technical considerations: CT viewing settings

Image reconstruction settings in 2-D MPR and 3-D rendering can also influence lesion visualization. Differences in the rendering algorithms used by different viewing software may affect the visibility of surface features (Khan et al., 2020). Horos' volume rendering, for instance, uses a ray tracing algorithm, while some viewers render 3-D images using ray marching. The specific effects of different algorithms on visualizing cranial porosity are unclear but worth considering.

The difference between slice thickness and axial resolution has counterintuitive effects on the visualization of cranial surface porosity. For the current study, resolution in axial images is approximately 0.39 mm^2, while resolution in the other planes is limited by the slice thickness of 0.63 mm. Given the finer axial resolution, one might conclude that the axial plane should provide the best visualization of porous lesions, but in 2-D reconstructions, surface porosity of the cranium's outer table is best visualized in a slice plane orthogonal to the layers of the cranial vault. Porosity in the superior cranial vault is therefore hard to identify in axial slices that run parallel/oblique to the layers of the calvarium, but axial resolution contributes to visualization of the superior cranial vault's outer table in 3-D renderings. In 2-D CT, axial images are best suited to capture porosity in the occipital squama.

Of course, viewing settings chosen by the observer will also impact lesion visibility, particularly in 3-D renderings, where the observer has more opportunities to customize settings. Multiple preset options exist within Horos and other DICOM viewers for window width and level, the color palette of rendered images, the algorithm used for calculating relative opacity of different density values, and the strength and diffusion of simulated light reflection from the tissue surface — and options also exist for entirely customized configurations (see Figs. S2 and S3). A single optimal setting configuration for viewing 3-D renderings of porous lesions has not been determined, but for moderate to severe lesions the range of settings used in this study do not appear to be a notable source of observer disagreement.

It is also worth noting that radiologists and osteologists may pick up on different skeletal features from the same images. In this study the radiologist's 2-D MPR assessments of lesion presence in the cranial vault are notably different from those of the osteologists, with far fewer false negatives (observer 4, Fig. 5A). It may be useful for a future study to compare scoring of multiple radiologists and osteologists to determine the effect of observer specialization on radiological assessments of paleopathological conditions, but it is likely that the majority of researchers interested in pursuing the evidence for porous cranial lesions in contemporary populations will continue to be osteologists. This result also suggests that osteologists might increase accuracy of assessments on 2-D MPR with radiological training.

3.5. A case for quantitative approaches

Despite general correlation between methods, there is considerable observer disagreement in lesion evaluations within viewing modalities. Across photographs, 2-D MPR, and 3-D CT, there was no case in which all observers agreed that vault lesions were absent. This may indicate an over-sensitivity on the part of observers due to the focus of the current study — availability bias or confirmation bias — though such sensitivity is likely a common variable in much research that relies on subjective evaluations of phenomena of interest.

Investigations of porous cranial lesions in living individuals will benefit from employing quantitative methods that minimize the impact of subjective evaluations. Since the raw data of a CT scan comprise a matrix of density values, such quantification is a natural approach to CT. For instance, hair-on-end appearance might be quantified as an entropy score of trabecular organization. Likewise, diploic granularity and porosity of the outer table, if they are visible to the trained eye, will also have signatures in the matrix of density data, and existing micro-CT work suggests that a range of disease processes might be identified based on quantitative differences in underlying trabecular architecture (Morgan, 2014). However, even quantitative analyses of porous cranial lesions using micro-CT found that, while differences in trabecular architecture could discriminate between unaffected orbits and those with moderate to severe lesions, subtler surface porosity was not associated with significant differences in underlying trabeculae (Morgan, 2014). Quantitative analysis of CT findings at multiple resolutions can produce an integrated understanding of shared patterns of pathophysiology across clinical and archaeological samples.

Some researchers have approached cranial thickness as a meaningful metric in evaluating lesions in archaeological crania, though the conclusions of these studies are limited either by their use of radiographs or by small sample sizes. Stuart-Macadam (1987) found consistent differences between crania with and without lesions in the ratio of cortical to diploic bone thickness. Likewise, Zuckerman et al. (2014) noted that among subadults with cranial lesions, individuals with lesions suggestive of scurvy had significantly thicker cranial vaults, though as scorbutic hemorrhage frequently leads to anemia it is difficult to draw a clear distinction between the skeletal manifestations of these conditions (Brickley et al., 2020: 241). Using a particularly sophisticated approach, River and Mirazon Lahr (2017) documented a complex relationship between orbital roof porosity and individual patterns of cranial vault

thickness. These studies suggest that a more comprehensive quantitative approach using CT scans is likely to yield productive and nuanced results about the covariation of osseous changes across the skull and the aspects of osseous change with most clinical significance.

4. Conclusion

Assessing the equivalence of evaluations of pathological skeletal lesions based on direct observation, photographs, and CT, we find that paleopathological criteria can be applied to standard cranial CTs to identify the presence of moderate to severe porous lesions of the cranial vault and to differentiate lesions with coalescing porosity from those with isolated foramina. Orbital roofs, however, are poorly visualized in standard head CT, and only extreme cases of cribra orbitalia are readily visible. Volume-rendered 3-D images are preferable for identifying lesion presence, but evaluation of lesion depth and morphology should be supported with cross-sectional views from 2-D MPR.

Based on these results, paleopathologists and radiologists can identify cranial vault lesions in living individuals on cranial CT scans, provided scans are obtained with a bone algorithm and submillimeter slice thickness and lesions a) present with more than pinprick porosity and b) lesion healing is not too advanced. Best practices might involve consensus by multiple observers in order to mitigate individual observer biases (Mays, 2020). As scanning technologies improve and hospitals continue to adopt 64-slice CT scanners in their trauma centers, cranial scans with submillimeter slice thickness is becoming routine for cases of head trauma (Mutch et al., 2016; Orman et al., 2015). The resolution of routine clinical imaging will only improve, closing the distance between findings from CT and direct observation of skeletal materials and expanding the opportunities for integrating paleopathological and clinical perspectives.

The application of comparable methods of data collection in clinical and archaeological cases has two major benefits for paleopathology. First, it serves to broaden the range of reference material for paleopathological diagnosis and thus mitigate some of the biases in skeletal profiles of disease that result from the unrepresentative nature of available reference cases (Mays, 2018). Second, it facilitates a lesion-centered approach to existing medical imaging from contemporary clinical cases, a program of research that can be undertaken by osteologists without requiring radiologists to reify and document skeletal findings that may be of minimal diagnostic relevance to identifying and treating a patient's condition. Such investigation of skeletal lesions in living individuals will simultaneously serve to test the diagnostic accuracy of paleopathological inference and explore the connection, beyond diagnosis, between skeletal manifestations of disease and individual disease experience.

We have provided here a case study of the groundwork needed to join paleopathological insights and existing clinical data by mapping out the strengths and limitations of clinical CT for examining an archaeologically defined pathological lesion. But there are still many open questions about porous cranial lesions that cannot be answered from archaeological samples, including their rate of remodeling, how commonly they are retained into adulthood, and the factors that determine both of these. Studying these lesions in living individuals as well as cases of lesion-associated ailments that present without cranial lesions will elucidate the conditions necessary to produce osseous changes and the aspects of disease experience that differ between those who develop skeletal lesions and those who do not. An integrated approach to skeletal pathology, enabled by the methods demonstrated here, will generate more meaningful analyses of disease in past populations and an unprecedented understanding of the relationship between health and the skeleton.

Funding

This research did not receive any specific grant from funding agencies in the public, commercial, or not-for-profit sectors.

Acknowledgements

Our deep gratitude to the Smithsonian's Division of Physical Anthropology for providing access to the skeletal materials and CT scanning using the Siemens SOMATOM Emotion 6 at the NMNH, donated by Siemens Healthineers. Heartfelt thanks to Andrew Nelson and our other knowledgeable reviewers for their thoughtful and thought-provoking feedback. And warm appreciation to Gabriella Campbell for help in the early stages of this project.

Appendix A. Supplementary data

Supplementary material related to this article can be found, in the online version, at doi:https://doi.org/10.1016/j.ijpp.2021.04.008.

References

Angel, J.L., 1964. Osteoporosis: thalassemia? Am. J. Phys. Anthropol. 22, 369–373.
Beatrice, J.S., Soler, A., 2016. Skeletal indicators of stress: a component of the biocultural profile of undocumented migrants in Southern Arizona. J. Forensic Sci. 61, 1164–1172. https://doi.org/10.1111/1556-4029.13131.
Beckett, R.G., 2014. Paleoimaging: a review of applications and challenges. Forensic Sci. Med. Pathol. 10, 423–436. https://doi.org/10.1007/s12024-014-9541-z.
Blom, D.E., Buikstra, J.E., Keng, L., Tomczak, P.D., Shoreman, E., Stevens-Tuttle, D., 2005. Anemia and childhood mortality: latitudinal patterning along the coast of pre-Columbian Peru. Am. J. Phys. Anthropol. 127, 152–169. https://doi.org/10.1002/ajpa.10431.
Brickley, M.B., 2018. Cribra orbitalia and porotic hyperostosis: a biological approach to diagnosis. Am. J. Phys. Anthropol. 167, 896–902. https://doi.org/10.1002/ajpa.23701.
Brickley, M.B., Ives, R., Mays, S., 2020. Biology and metabolism of mineralised tissues. The Bioarchaeology of Metabolic Bone Disease, pp. 23–41. https://doi.org/10.1016/b978-0-08-101020-4.00003-3.
Buikstra, J.E., Ubelaker, D.H., 1994. In: Standards for Data Collection from Human Skeletal Remains: Proceedings of a Seminar at the Field Museum of Natural History. Arkansas Archeological Survey, Fayetteville, AR.
Clini, P., Frapiccini, N., Mengoni, M., Nespeca, R., Ruggeri, L., 2016. SFM technique and focus stacking for digital documentation of archaeological artifacts. Int. Arch. Photogramm. Remote Sens. Spat. Inf. Sci. - ISPRS Arch. 41, 229–236. https://doi.org/10.5194/isprsarchives-XLI-B5-229-2016.
Conlogue, G.J., Nelson, A.J., Lurie, A.G., 2020. computed tomography (CT), multi-detector computed tomography (MDCT), micro-CT, and cone beam computed tomography (CBCT). In: Conlogue, G., Beckett, G. (Eds.), Advances in Paleoimaging: Applications for Paleoanthropology, Bioarchaeology, Forensics, and Cultural Artifacts. CRC Press, Abingdon, pp. 111–178.
David, M., 2018. Traumatic Predictors of Femicide: a Forensic Anthropological Approach to Domestic Violence. Florida Gulf Coast University.
DeWitte, S.N., Stojanowski, C.M., 2015. The osteological paradox 20 years later: past perspectives, future directions. J. Archaeol. Res. 23, 397–450. https://doi.org/10.1007/s10814-015-9084-1.
Exner, S., Bogusch, G., Sokiranski, R., 2004. Cribra orbitalia visualized in computed tomography. Ann. Anat. 186, 169–172. https://doi.org/10.1016/S0940-9602(04)80035-9.
Goldman, L.W., 2008. Principles of CT: multislice CT. J. Nucl. Med. Technol. 36, 57–68. https://doi.org/10.2967/jnmt.107.044826.
Hassan, B., Van Der Stelt, P., Sanderink, G., 2009. Accuracy of three-dimensional measurements obtained from cone beam computed tomography surface-rendered images for cephalometric analysis: influence of patient scanning position. Eur. J. Orthod. 31, 129–134. https://doi.org/10.1093/ejo/cjn088.
Horos, 2019. Horos.
Hrdlička, A., 1914. Anthropological work in Peru in 1913, with notes on the pathology of the ancient Peruvians. Smithson. Misc. Collect. 61, 1–69.
Józsa, L., Pap, I., 1990. Morphology and differential diagnosis of porotic hyperostosis on historical anthropological material. Anthropol. Hungarica 21, 69–80.
Khan, U., Khan, U., Yasin, A., Shafi, I., Abid, M., 2020. CPU-GPU rendering of CT scan images for vertebra reconstruction from CT scan images with a calibration policy. Med. Imaging Radiat. Sci. 1–5. https://doi.org/10.31487/j.mirs.2020.01.02.
Lewis, M.E., 2017. Paleopathology of Children: Identification of Pathological Conditions in the Human Skeletal Remains of Non-Adults. Elsevier Inc., London.
Maetani, K., Namiki, J., Matsumoto, S., Matsunami, K., Narumi, A., Tsuneyoshi, T., Kishikawa, M., 2016. Routine head computed tomography for patients in the emergency room with trauma requires both thick- and thin-slice images. Emerg. Med. Int. 2016. https://doi.org/10.1155/2016/5781790.
Mays, S., 2012. The relationship between paleopathology and the clinical sciences. In: Grauer, A.L. (Ed.), A Companion to Paleopathology. Wiley-Blackwell, West Sussex, pp. 285–309. https://doi.org/10.1002/9781444345940.ch16.

Mays, S., 2018. How should we diagnose disease in palaeopathology? Some epistemological considerations. Int. J. Paleopathol. 20. https://doi.org/10.1016/j.ijpp.2017.10.006.
Mays, S.A., 2020. A dual process model for paleopathological diagnosis. Int. J. Paleopathol. 31, 89–96. https://doi.org/10.1016/j.ijpp.2020.10.001.
McCollough, C.H., 2011. Translating protocols between scanner manufacturer and model. Technology Assessment Initiative: Summit on CT Dose.
Meindl, R.S., Lovejoy, C.O., 1985. Ectocranial suture closure: a revised method for the determination of skeletal age at death based on the lateral-anterior sutures. Am. J. Phys. Anthropol. 68, 57–66.
Mensforth, R.P., Lovejoy, C.O., Lallo, J.W., Armelagos, G.J., 1978. Part two: the role of constitutional factors, diet, and infectious disease in the etiology of porotic hyperostosis and periosteal reactions in prehistoric infants and children. Med. Anthropol. 2, 1–59. https://doi.org/10.1080/01459740.1978.9986939.
Morgan, J., 2014. The Methodological and Diagnostic Applications of Micro-CT to Palaeopathology : A Quantitative Study of Porotic Hyperostosis. The University of Western Ontario.
Mutch, C.A., Talbott, J.F., Gean, A., 2016. Imaging evaluation of acute traumatic brain injury christopher. Physiol. Behav. 176, 139–148. https://doi.org/10.1016/j.physbeh.2017.03.040.
Naveed, H., Abed, S.F., Davagnanam, I., Uddin, J.M., Adds, P.J., 2012. Lessons from the past: cribra orbitalia, an orbital roof pathology. Orbit 31, 394–399. https://doi.org/10.3109/01676830.2012.723785.
O'Donnell, L., 2019. Indicators of stress and their association with frailty in the pre-contact southwestern United States. Am. J. Phys. Anthropol. 170, 404–417. https://doi.org/10.1002/ajpa.23902.
O'Donnell, L., Hill, E.C., Anderson, A.S., Edgar, H.J.H., 2020. Cribra orbitalia and porotic hyperostosis are associated with respiratory infections in a contemporary mortality sample from New Mexico. Am. J. Phys. Anthropol. 173, 721–733. https://doi.org/10.1002/ajpa.24131.
Obertova, Zuzana, Thurzo, M., 2004. Cribra orbitalia as an indicator of stress in the early medieval Slavic population from Borovce (Slovakia). Anthropologie 42, 189–194.
Orman, G., Wagner, M.W., Seeburg, D., Zamora, C.A., Oshmyansky, A., Tekes, A., Poretti, A., Jallo, G.I., Huisman, T.A.G.M., Bosemani, T., 2015. Pediatric skull fracture diagnosis: should 3D CT reconstructions be added as routine imaging? J. Neurosurg. Pediatr. 16, 426–431. https://doi.org/10.3171/2015.3.PEDS1553.
Ortner, D.J., 2003. Identification of Pathological Conditions in Human Skeletal Remains, 2nd ed. Academic Press, San Diego.
Ortner, D.J., Ericksen, M.F., 1997. Bone changes in the human skull probably resulting from scurvy in infancy and childhood. Int. J. Osteoarchaeol. 7, 212–220.
Resnick, D., Niwayama, G., 1988. Diagnosis of bone and joint disorders. Saunders, Philadelphia.
Rivera, F., Mirazon Lahr, M., 2017. New evidence suggesting a dissociated etiology for cribra orbitalia and porotic hyperostosis. Am J Phys Anthr. 164, 76–96. https://doi.org/10.1002/ajpa.23258.
Rosel, P., 2015. The basics of orbital imaging. In: Karcioglu, Z.A. (Ed.), Ed.), Orbital Tumors: Diagnosis and Treatment. Springer, New York, pp. 83–95. https://doi.org/10.1007/978-1-4939-1510-1_9.
Steckel, R.H., Rose, J.C., Larsen, C.S., Walker, P.L., 2002. Skeletal health in the western hemisphere from 4000 B.C. To the present. Evol. Anthropol. 11, 142–155. https://doi.org/10.1002/evan.10030.
Steyn, M., Voeller, S., Botha, D., Ross, A.H., 2016. Cribra orbitalia: prevalence in contemporary populations. Clin. Anat. 830, 823–830. https://doi.org/10.1002/ca.22734.
Stuart-Macadam, P., 1985. Porotic hyperostosis: representative of a childhood condition. Am. J. Phys. Anthropol. 66, 391–398. https://doi.org/10.1002/ajpa.1330660407.
Stuart-Macadam, P., 1987. Porotic Hypertostosis: new evidence to support the anemia theory. Am. J. Phys. Anthropol. 74, 521–526.
Stuart-Macadam, P., 1987. A radiographic study of porotic hyperostosis. Am. J. Phys. Anthropol. 74, 511–520. https://doi.org/10.1002/ajpa.1330740409.
Ubelaker, D.H., 2003. Anthropological perspectives on the study of ancient disease. In: Greenblatt, C., Spigelman, M. (Eds.), Emerging Pathogens, Archaeology, Ecology and Evolution of Infectious Disease. Oxford University Press, Oxford, pp. 93–102.
Waldron, T., 2009. Paleopathology. Cambridge University Press, Cambridge.
Walker, P.L., Bathurst, R.R., Richman, R., Gjerdrum, T., Andrushko, V.a, 2009. The causes of porotic hyperostosis and cribra orbitalia: a reappraisal of the iron-deficiency-anemia hypothesis. Am. J. Phys. Anthropol. 139, 109–125. https://doi.org/10.1002/ajpa.21031.
Wapler, U., Crubézy, E., Schultz, M., 2004. Is cribra orbitalia synonymous with Anemia? Analysis and interpretation of cranial pathology in Sudan. Am. J. Phys. Anthropol. 123, 333–339. https://doi.org/10.1002/ajpa.10321.
Watts, R., 2013. Childhood development and adult longevity in archaeological populations from Barton-upon-Humber, Lincolnshire. England. Int. J. Paleopathol. 3, 95–104.
Wood, J.W., Milner, G.R., Harpending, H.C., Weiss, K.M., Cohen, M.N., Eisenberg, L.E., Hutchinson, D.L., Jankauskas, R., Česnys, G., Katzenberg, M.A., Lukacs, J.R., Mcgrath, J.W., Roth, A., Ubelaker, D.H., Wilkinson, R.G., Wood, J.W., Milner, G.R., Harpending, H.C., Weiss, K.M., 1992. The osteological paradox : problems of inferring prehistoric health from skeletal samples. Curr. Anthropol. 33, 343–370.
Wright, L.E., Chew, F., 1998. Porotic hyperostosis and paleoepidemiology: a forensic perspective on Anemia among the ancient maya. Am. Anthropol. 100, 924–939. https://doi.org/10.1525/aa.1998.100.4.924.
Zuckerman, M.K., Garofalo, E.M., Frohlich, B., Ortner, D.J., 2014. Anemia or scurvy : a pilot study on differential diagnosis of porous and hyperostotic lesions using differential cranial vault thickness in subadult humans. Int. J. Paleopathol. 5, 27–33. https://doi.org/10.1016/j.ijpp.2014.02.001.